BUTTERWORTH HEINEMANN

Polymer Vol. 36 No. 19, pp. 3649–3659, 1995
Elsevier Science Ltd
Printed in Great Britain
0032-3861/95/$10.00 + 0.00

Influence of siloxane composition and morphology on properties of polyimide–silica hybrids

L. Mascia* and A. Kioul
Institute of Polymer Technology and Materials Engineering, Loughborough University of Technology, Loughborough LE11 3TU, UK
(Received 7 November 1994; revised 10 February 1995)

Hybrid organic–inorganic materials based on polyimide–silica systems have been produced by the sol–gel route from solution mixtures of hydrolysed tetraethoxysilane (TEOS) and an aromatic polyamic acid. Compatibilization of the two components was achieved with the addition of small amounts of γ-glycidyloxypropyltrimethoxysilane, and the evolution of the morphology was controlled by the partial substitution of TEOS with dimethylethoxysilane. In all cases imidization and network formation for the two respective components were carried out simultaneously on cast films after evaporating the solvent through successive temperature rises in steps up to a maximum of 300°C. The results illustrate the role of the interconnected silica-rich particles within the polyimide-rich matrix in depressing the α-relaxations and reducing accordingly the thermal expansion coefficient of the film or coating by an extent substantially greater than can be expected from the usual additivity rules. Forcing the reoccurrence of a particulate morphology through desolubilization of the siloxane component and simultaneously preserving the adhesion between the two phases gives rise to substantial improvements in both tensile strength and elongation at break. For systems exhibiting a co-continuous two-phase morphology the observed changes in properties can be partially attributed to residual orientation within the polyimide phase resulting from the internal constraints imposed on its shrinkage during removal of the solvent and the imidization reactions.

(Keywords: siloxanes; polyimide–silica hybrids; morphology)

INTRODUCTION

A considerable amount of research has been carried out since the mid-1970s on sol–gel processing of metal oxides to produce ceramics and glasses of high purity[1–3]. Owing to the excessive volumetric shrinkage that takes place during drying, the sol–gel process is primarily used for the production of multicomponent systems in the form of powders[4–6], fibres[7,8] and coatings[9,10]. Although sol–gel processing of ceramics and glasses can be carried out through the gelation of a solution of colloidal powders, the process that has received the greatest attention makes use of alkoxide precursors. The general sol–gel reaction scheme can be viewed as a two-step process in which the metal alkoxide≡MOR is hydrolysed to generate intermediate species≡MOH which will then form three-dimensional networks through condensation reactions. The liquid phase is subsequently removed by thermal evaporation to produce a porous material with pore dimensions less than 10 nm and a surface area greater than 400 m^2g^{-1}, giving a pore volume ca. 30–50% of the total.

The microstructure of the porous metal oxide obtained by the sol–gel process is dependent on the kinetics of the hydrolysis and condensation reactions, which are largely controlled by the pH of the solution[11–13], the water to metal alkoxide ratio[14], the type of solvent and the nature of the alkoxy groups[15,16]. Chemical stability of dried gels is achieved by removing the chemisorbed hydroxy groups from the surface of the pores through thermal treatment at around 500–800°C. Heating the dried gels at higher temperatures causes densification through collapse of the pores by viscous flow[17].

The types of reactions involved in the sol–gel process make it possible to produce intimate mixtures of organic polymers and inorganic glasses by preventing premature phase separation. This is achievable by promoting reactions or strong physical interactions between the two components, either directly or via a 'coupling' agent. Owing to the high degree of condensation in the production of alkoxide networks by the sol–gel process, the heat treatment steps normally used for the production of glasses or ceramics can be omitted, so that the resulting hybrid will exhibit properties that fall between those of polymers and ceramics.

Wilkes and coworkers[18,19] were among the first to exploit this concept by producing hybrids, which they called 'ceramers', from solution mixtures of tetraethoxysilane (TEOS) and hydroxy-terminated oligomers based on dimethylsiloxane (PDMS) and tetramethylene oxide (PTMO), respectively. By altering the molecular weight and functionality of the oligomer and the concentrations of the organic and inorganic components, these authors were able to produce ceramers with different properties, ranging from soft elastomers to hard or ductile plastics. Small angle X-ray diffraction analysis showed that the

* To whom correspondence should be addressed

silica component formed clusters which increased in size with increasing TEOS concentration in the sol.

In the work carried out on hybrids based on zirconia–PTMO and titania–PTMO, Wilkes *et al.*[20] found that unlike the silica-based ceramers, these systems exhibited sharp boundaries between the two phases. The Young's modulus and stress at break of the ceramers were much higher when either zirconia or titania was used instead of silica.

Research on polyimide–silica hybrids was first reported in the early 1990s. Nandi *et al.*[21,22] have produced polyimide–metal oxide hybrid materials by mixing solutions of pyromellitic anhydride (PDMA), diaminodiphenyl ether (ODA) and either titanium or silicon tetraalkoxides. The reaction mixture was cast into films and heated to 300°C.

Spinu *et al.*[23] produced silica ceramers by mixing solutions of methoxysilane-terminated polyimide oligomers and tetraethoxysilane, whereas Morikawa *et al.*[24,25] used mixtures of a polyamic acid containing pendant alkoxysilane groups along the chains with tetraethoxysilane, subsequently effecting the imidization and advancing the condensation reactions in the siloxane network by heating the films in steps to 300°C.

Mascia and Kioul[26,27] have reported the use of functionalized alkyltriethoxysilanes to 'couple' a polyamic acid to the silicate network prior to the condensation reactions for the formation of the ceramer. By varying the composition and mixing conditions a range of morphologies were obtained ranging from interpenetrating networks (IPNs) to finely dispersed particles.

In this paper we consider the means of achieving further morphological transformations by reducing the miscibility of the alkoxysilane component in polyimide–silica hybrids and examine the manner in which these transformations affect mechanical properties and thermal expansion behaviour. The latter analysis takes into consideration the effects of residual moisture and the constraints on the films during the simultaneous imidization of the polyamic acid and the polycondensation of the tetraethoxysilane component.

EXPERIMENTAL

Materials

The polyamic acid (polyimide precursor) mostly used in this study was the high molecular weight Pyre ML RK692 (Du Pont), available as a 14% solution in a mixture of *N*-methyl-2-pyrrolidone (NMP) and xylene.

A small number of ceramer films were produced using the low molecular weight polyamic acid Skybond 703 (Monsanto), available as a 65% solution in a mixture of *N*-methyl-2-pyrrolidone and ethanol. The structures of the two polyamic acids used and the equation for the imidization reaction are

Pyre ML Polyamic Acid

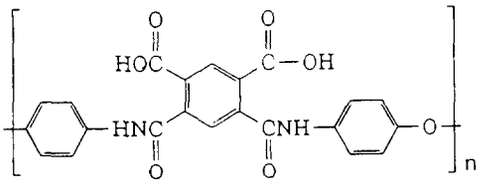

Skybond 703 Polyamic Acid

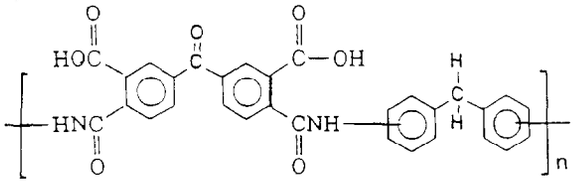

Imidisation Reaction

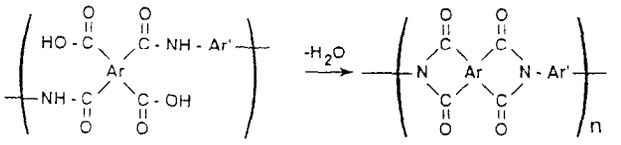

High purity grades of tetraethoxysilane (TEOS) and γ-glycidyloxypropyltrimethoxysilane (GOTMS) were obtained from Fluka, while dimethyldiethoxysilane (DMES) was purchased from Fluorochem. Distilled water was used to induce the hydrolytic reactions in the alkoxysilane components using a 32% (w/w) HCl solution as catalyst and ethanol as solvent.

Film preparation

The alkoxysilane solutions used for the production of polyimide–silica hybrid films were prepared from either pure TEOS or TEOS–GOTMS mixtures containing varying amounts of DMES as a network modifier. The compositions of the alkoxysilane solutions are detailed in *Table 1*.

All the alkoxysilane solutions were 'prepolymerized' in a closed system at room temperature for 16 h and subsequently mixed with the polyamic acid solution in varying amounts to produce ceramer solutions. The prepolymerization of the alkoxysilane solution proceeds as in *Scheme 1*.

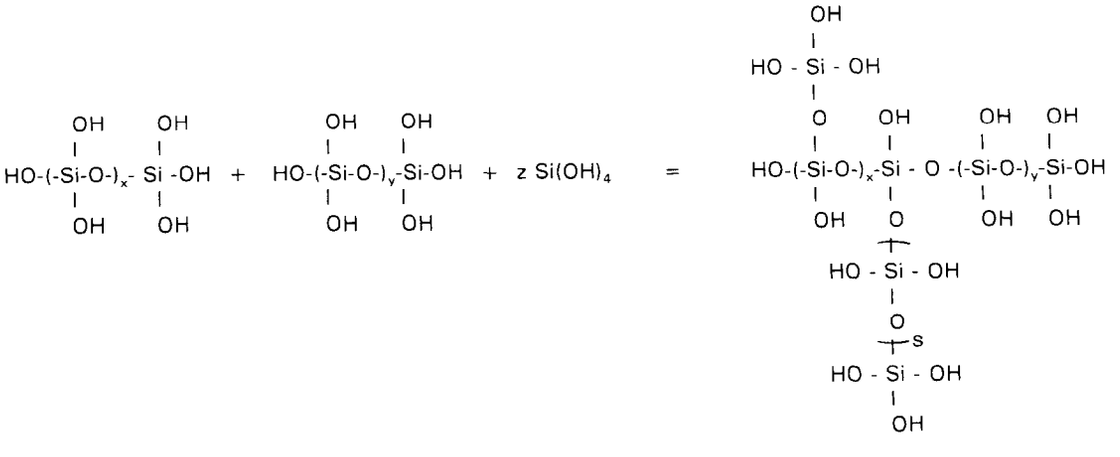

Scheme 1

Table 1 Alkoxysilane solutions based on TEOS, TEOS–GOTMS and TEOS–GOTMS–DMES

	DMES to TEOS molar ratio	TEOS (mol)	DMES (mol)	GOTMS (mol)	H_2O (mol)	HCl (mol)	C_2H_5OH (mol)
S	0	1.0	0	0	2.20	0.05	1.10
SE_2	0	1.0	0	0.12	3.20	0.05	1.13
D_5E_2	0.125	1.0	0.125	0.12	4.80	0.06	0.88
D_4E_2	0.25	1.0	0.25	0.12	4.90	0.07	0.88
D_3E_2	0.5	1.0	0.50	0.12	5.00	0.06	0.93
D_2E_2	1.0	1.0	1.00	0.12	5.50	0.07	1.70

The hydrolysis and condensation reactions occur at various sites within the TEOS–H_2O solution. When sufficient branched siloxane groups are formed the products of the reaction behave as aggregated domains (sol) whose size and density depend on the pH. When the coupling agent is used the three methoxy groups will hydrolyse and produce a network through co-condensation reactions with the rest of the silanol groups from TEOS. At the same time some

$$CH_2 - CH - CH_2 - O - (CH_2)_3 - Si\equiv$$
$$\quad\ \backslash\ /$$
$$\quad\ \ O$$

units can form an interpenetrating network through self-addition reactions of the epoxy groups[27]. The incorporation of DMES, on the other hand, is expected to reduce the network density.

These solutions were reacted by stirring at 80 rev min^{-1} for different times in a glass beaker (open system) immersed in an oil bath maintained at 80°C. The ceramer solutions and the polyamic acid solution treated in the same manner (control) were then cooled down to room temperature and subsequently cast as thin films (40–60 μm) on glass plates and dried at 80°C for 0.5 h. Attempts to produce films from one-component alkoxide solutions were aborted owing to their excessive brittleness. Curing of the ceramer films was carried out by successive 1 h heating steps at 100, 150, 200, 250 and 300°C. This induced imidization of the polyamic acid and crosslinking of the siloxane component.

Morphology of ceramers. The fractured surfaces of films obtained after cooling in liquid nitrogen were examined on a Cambridge 360 stereoscan electron microscope.

Coefficients of thermal expansion. The mean values of the linear coefficient of thermal expansion (CTE) were obtained from measurements on a Mettler TA 4000 apparatus at a heating rate of 10°C min^{-1} from room temperature to 350°C. Films were normally produced on glass slides by spreading the solution, drying for 1 h at 80°C and 100°C, respectively, peeling the films from the substrate and subjecting them to the stepwise heat treatment outlined earlier.

A number of model experiments were carried out on non-modified polyimide films to determine the effect of performing the imidization reaction under biaxial constraints. This was established by heating the film respectively under compression between two plates and on adhering substrates. In the latter case the relative importance of the surface energy of the substrate during both drying and imidization was determined by using glass slides and a crystalline poly(arylene ether ketone) (PEEK) as substrates, whose surface energies are in the region of 70 mJ m^{-2} and 40 mJ m^{-2}, respectively*. Thermal expansion measurements were also made on films imidized at temperatures less than 300°C both in the free state and on glass slides to study the effects of varying levels of molecular relaxation. To examine the effects of residual water the temperature was cycled at a constant rate of 10°C min^{-1} up to the desired imidization temperature. For all other experiments the samples were dried by cycling the temperature from room temperature to 250°C, i.e. below the T_g of the material, before readings were taken.

Mechanical properties. Except for films that were heat treated on a supporting substrate, the specimens were punched out from dried films and then heat treated in the free state. Small dumb-bell specimens with waist dimensions of 25 × 5 mm were used for the tensile tests. Stress and extension measurements were made at room temperature on a J. J. Lloyd machine with a cross-head speed of 2 mm min^{-1} and dynamic mechanical spectra were obtained on Polymer Laboratories apparatus at 5 Hz with a temperature scan rate of 5°C min^{-1} up to 500°C.

RESULTS AND DISCUSSION

Morphology of ceramers

The scanning electron micrographs in *Figures 1* and *2* show clearly the miscibilization of polyimide–silica mixtures by the addition of small amounts of γ-glycidyloxypropyltrimethoxysilane (GOTMS) to the tetraethoxysilane (TEOS) solution used for the production of polyimide ceramers, which brings about a morphological transformation from a dispersed particle microstructure (*Figures 1a* and *2a*) to fine interconnected or co-continuous phases (*Figures 1b* and *2b*). Partially substituting TEOS with DMES, on the other hand, promotes a reversion of the morphology to disconnected particles (*Figures 2c* and *2d*). In this case, however, the dimensions of the particles are always smaller than in the absence of the coupling agent. The micrographs in *Figure 3* illustrate also that compatibilization results from chemical reactions between polyamic acid and the coupling agent present in the siloxane component. It is seen that the dispersed silica particles after 2 h of mixing are much smaller than those at very short mixing times.

At the same time the micrographs reveal that in systems where dispersed particles are present, i.e. the non-compatibilized ceramers and those containing DMES, the size of the particles is uniform. This has been given by other authors[28,29] as evidence of phase separation by spinodal decomposition.

Previous work on polyimide–silica hybrids reported elsewhere[27] has shown that no further changes in morphology take place in the subsequent heating steps to take condensation reactions in the two components to completion and to eliminate final traces of solvents. At

* Values recorded after cleaning the surface in NMP and drying in an oven at 200°C

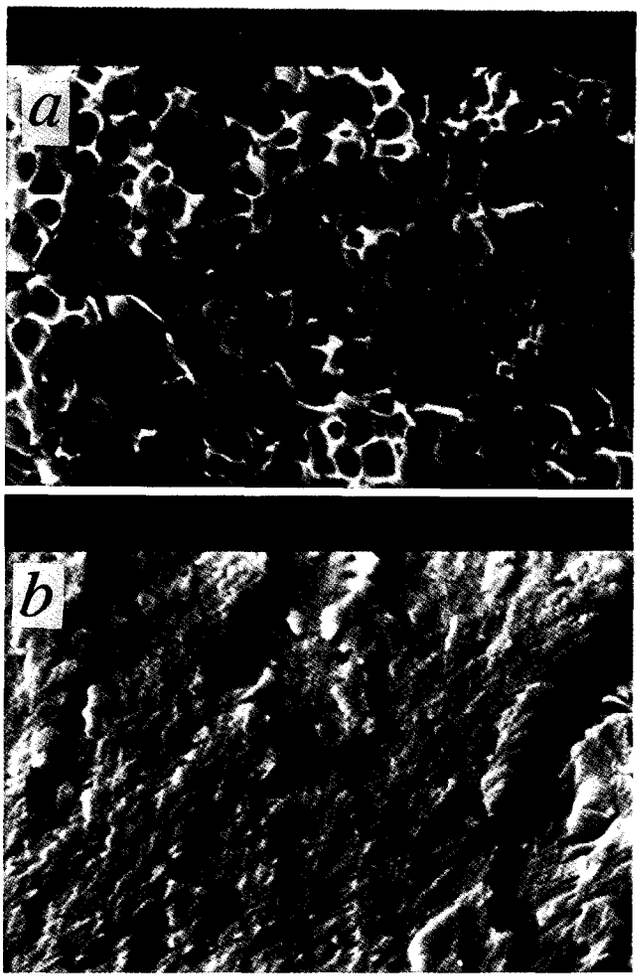

Figure 1 Scanning electron micrographs of fractured surfaces of ceramers (25% (w/w) SiO_2) based on a low molecular weight polyimide (Skybond 703) and mixed for 1 h at 80°C: (a) ceramer film without coupling agent; (b) ceramer film containing 10% (molar) GOTMS with respect to silica content

the same time, while the extent of imidization was found not to be affected by the presence of the siloxane component, it has not been possible to reach any conclusion regarding the porosity of the silica phase. On the other hand, the rate of gelation of the silica sol was found to increase upon addition of the GOTMS coupling agent and to decrease when TEOS was partially replaced with DMES. Taking these observations in conjunction with the morphologies revealed in *Figures 2* and *3*, a scenario can be constructed for the manner in which the coupling agent induces and controls the evolution of a co-continuous two-phase morphology. In the mixing of the two solutions, reactions take place between the epoxy groups from the coupling agent in the siloxane and the acid groups of the polyimide precursor to produce *in situ* a compatibilizer for the two components. This has the effect of retarding the phase separation process when the solvent is evaporated, i.e. it reduces the quantity of solvent required to maintain homogeneity. At the same time the increased rate of gelation of the siloxane component brought about by the addition of the coupling agent[27] causes a slowing down of the phase-coarsening process which follows the spinodal decomposition, thereby preventing the breaking up of the co-continuity of the minor silica phase before the onset of gelation which freezes the microstructure. The shorter periodic distance (i.e. finer domains) for the ceramers obtained with the lower molecular weight polyamic acid results from the greater miscibility of this acid, which retards the onset of spinodal decomposition (i.e. it occurs at a lower content of residual solvent and at a more advanced state of the condensation reactions in the two components) and reduces the rate of phase coarsening.

The formation of discrete particles, on the other hand, when DMES is used as a partial replacement for TEOS in the siloxane solution can be explained in terms of two effects. Firstly, the reduction in gelation rate, as mentioned earlier, allows the breaking up of the co-continuity of the phases to reach a more advanced state of phase separation before the onset of gelation. Secondly, the presence of the more hydrophobic DMES reduces the solubility of the siloxane phase and brings forward the occurrence of spinodal decomposition during solvent evaporation. The deterioration of the solubility characteristics of the siloxane component with increasing amount of DMES used in the production of the sol was confined in the preliminary studies to determine the maximum possible DMES to TEOS molar ratio.

The size of the particles growing out of the spinodal phase separation process, however, remains quite small (*Figure 3b*) in view of the lower rate with which particles can grow out of the compatibilized siloxane–polyamic acid mixture. In other words, the stronger physical interactions and higher level of entanglements due to the presence of graft reaction products are expected to reduce the rate of molecular diffusion across the phase boundaries.

In examining the micrograph of *Figure 3b* one notes that although a considerable level of interfacial cavitation has taken place, there are a number of webs connecting the silica gel particles to the surrounding polyimide matrix. Since these are absent in systems produced with a very short mixing time (*Figure 3a*), where the reactions between polyamic acid and the epoxy groups of the coupling agent have not taken place, it can be inferred that the webs result from the strong adhesion between the two phases, giving rise to ductile tearing of the polyimide phase around the silica particles.

Mechanical properties

Dynamic mechanical tests. Typical mechanical relaxation spectra for the ceramers and the parent polyimide (Pyre ML) are shown in *Figure 4*. The observations that can be made on these data are as follows.

1. Compatibilization of polyimide ceramers to produce a co-continuous two-phase morphology brings about a large depression of the α-relaxations. Although there are considerable errors in the recorded values for the elastic modulus (E') in the glassy state regions, a much higher level of reinforcement is evident for the same systems at temperatures above the glass transition. It is worth noting that from wide angle X-ray diffraction and dilatometry experiments it has been confirmed that the upturn in the E' curve above the peak $\tan\delta$ temperature does not arise from crystallization of the polyimide, but it is likely to be the result of intermolecular crosslinking reactions.

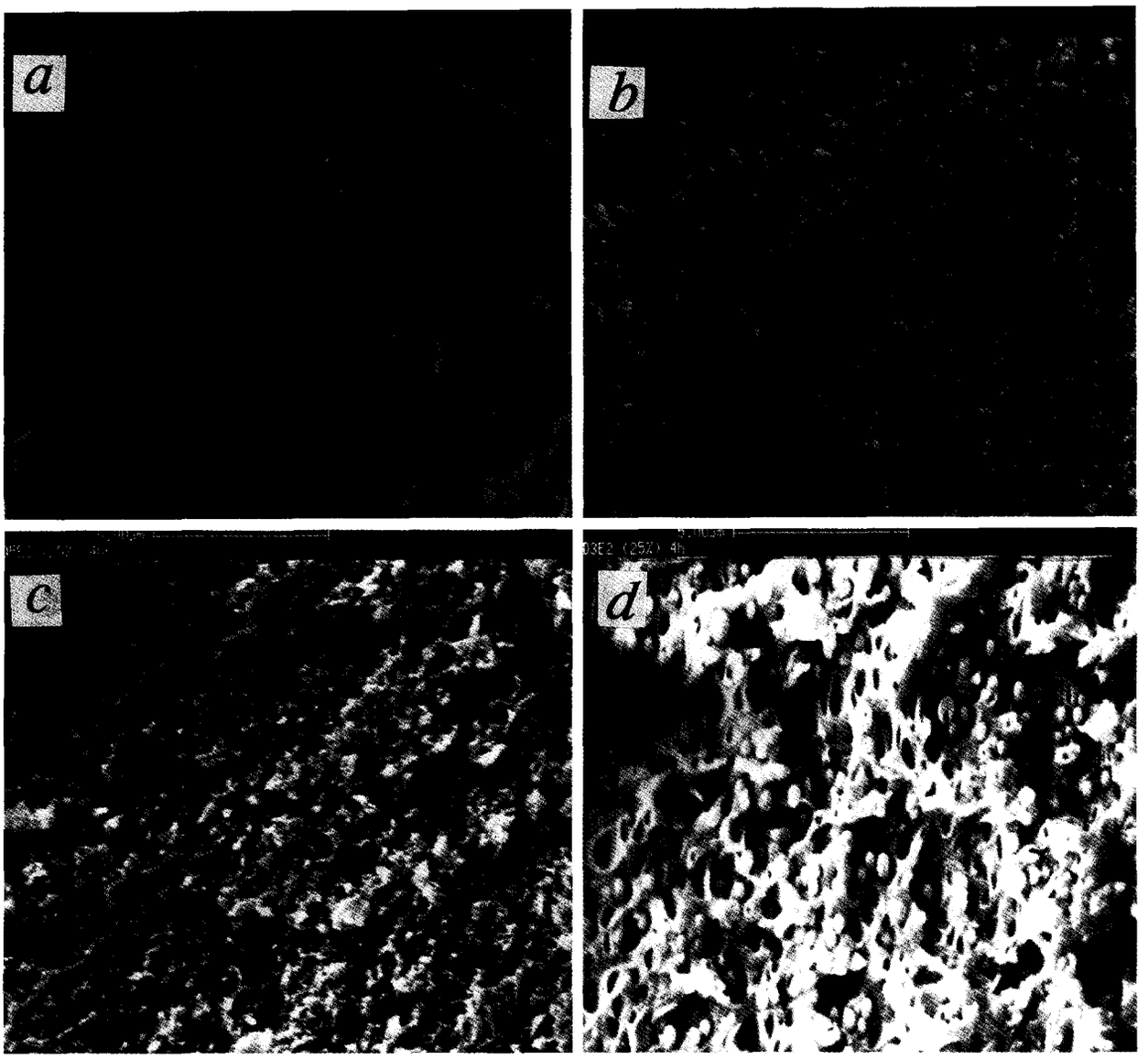

Figure 2 Scanning electron micrographs of polyimide ceramers with a silica content equivalent to 25% (w/w) SiO_2 (the compositions of the precursor alkoxysilane solutions are shown in *Table 1*): (a) ceramer S–Pyre ML; (b) ceramer SE_2–Pyre ML (alkoxy solution prepolymerized for 4 h at 80°C before casting into film); (c) ceramer D_5E_2–Pyre ML; (d) ceramer D_3E_2–Pyre ML (alkoxy solution prepolymerized for 4 h at 80°C before casting into film)

2. The peak tan δ temperature generally increases by ca. 10–15°C from that of the parent polyimide with the incorporation of an equivalent SiO_2 content of 25–35% (w/w). Taken in conjunction with the data on thermal expansion measurements (see later), this is sufficient evidence for an increase in glass transition temperature.
3. The peak tan δ values for the non-compatibilized ceramers are approximately equal to the values calculated from simple additivity rules assuming that the precipitated silica particles are elastic and that interfacial losses are negligible. For compatibilized ceramers, on the other hand, the experimental peak tan δ values are considerably lower. By assuming that the continuous silica phase is elastic, the calculated lower bound values at the peak of the tan δ curve are approximately 0.16 and 0.15 for equivalent SiO_2 contents of 25 and 35% (w/w), respectively, while the corresponding experimental values lie in the ranges 0.10–0.125 and 0.08–0.09.

Whereas it can be argued that the tan δ values recorded in dynamic tests are not directly proportional to the true energy losses but to losses normalized with respect to the elastic energy, they can nevertheless be taken as indicators of the relative changes in the viscoelastic nature of the material. Hence, while the equivalence of peak tan δ values to those calculated from a simple law of mixtures for systems containing co-continuous phases is not accurate, the relative comparisons are valid and informative. It is possible to deduce, therefore, that the large discrepancy in tan δ values in relation to those calculated empirically by the additivity rule is indicative of the involvement of polyimide chains in the silicate network through the coupling of the two components by the GOTMS. For instance, when the films are postcured

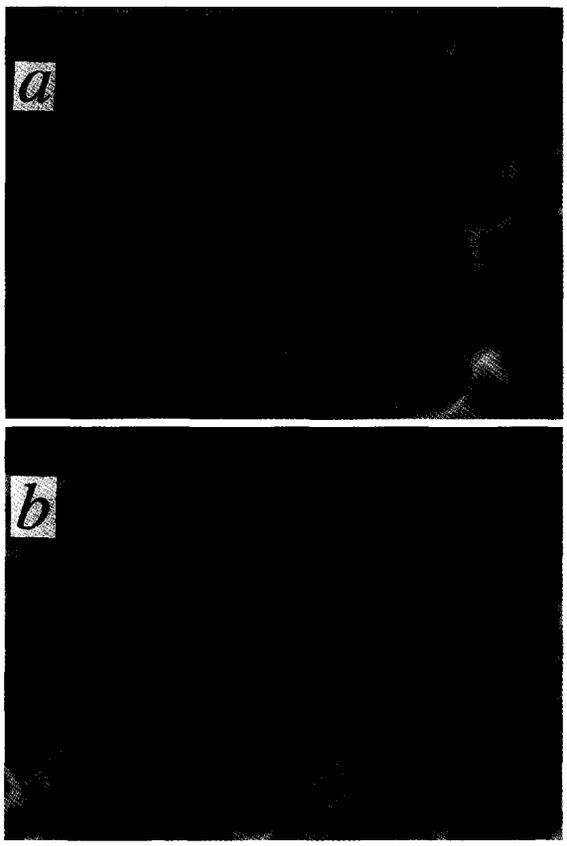

Figure 3 Effect of duration of mixing of the polyamic acid and tetraethoxysilane solution for system D_2E_2 (composition shown in *Table 1*). Scanning electron micrographs of fractured surfaces of imidized films: (a) mixing time 1 min; (b) mixing time 2 h

for 0.5 h at 400°C the peak tan δ value decreases from 0.195 to 0.10 for the polyimide and from 0.125 to 0.05 for the ceramer SE_2 containing 25% (w/w) equivalent SiO_2. The reduction is proportionally much greater for ceramers than for polyimides. Appreciable reductions in peak tan δ values, typically from 0.125 to 0.08–0.10, have also been found when the mixing time of the ceramer solution was increased from 2 to 4 h prior to casting the films, thereby confirming the effect of chemical reactions between the two phases (see also *Figure 4*).

Although not shown in *Figure 4* it is worth noting that the partial replacement of TEOS with DMES results in a substantial increase in peak tan δ values. For instance, the peak tan δ value for ceramer D_3E_2 (i.e. a molar ratio of DMES to TEOS of 0.5) after postcuring at 400°C was ca. 0.085 against a typical value of ca. 0.06 for the equivalent ceramer without DMES. It is difficult to say, however, whether the difference arises entirely from the change in morphology or whether there is also a contribution to the total losses from the siloxane phase as a result of the reduction in crosslinking density.

Tensile tests. The results of the tensile tests, expressed as tensile strength and elongation at break, are shown in *Figure 5*. Only the ceramers based on the high molecular weight polyimide were evaluated. In all cases, including the polyimide samples which exhibited elongation at break values in the region of 35%, there was no sign of cold drawing in the failure regions and no maxima or plateaux in the force–extension curves recorded. The increase in tensile strength resulting from the development of a co-continuous phase morphology with the addition of the GOTMS coupling agent can obviously be attributed to a more efficient stress transfer mechanism between the two components. The reduction in tensile strength occurring at SiO_2 contents greater than 25% (w/w) for the compatibilized systems SE_2 and at less than 10% (w/w) for the non-compatibilized systems can be attributed to the notch sensitivity of the polyimide. The larger domains of the silica gel phase and the lack of interfacial adhesion for the non-compatibilized systems can be considered to have an effect equivalent to that of larger defects.

The elongation at break, on the other hand, decreases about equally in the two cases with increasing silica content, confirming that failure is controlled mainly by events within the polyimide phase. The increase in T_g identified for both types of ceramers suggests that the polyimide phase always contains small amounts of siloxane networks formed as a result of the spinodal decomposition from the precursor solution. These networks will restrict the movements of the polyimide chains, thereby preventing the occurrence of large macroscale extensions. In other words, whereas the magnitude of the stresses in the polyimide phase at the point of failure is determined by the level of reinforcement provided by the silica phase, the value of the principal strain (elongation) at break is controlled by the incidental molecular structure modifications of the matrix.

In *Figure 6* it is shown that the partial replacement of TEOS with DMES in compatibilized hybrids, on the other hand, brings about an increase in both tensile strength and elongation at break, leading to a deterioration in these properties at higher substitution levels. A similar observation has been reported by Iyoku *et al.*[30] for polyimide hybrids in which the methyltriethoxysilane (MTES) component was partially replaced with DMES. Furthermore, higher elongation at break values were obtained when films were cast from methanol rather than dimethylacetamide solutions. These observations suggest that the effects may be due to a reduction in solubility of the oligomeric siloxane components in the polyimide, and possibly also to a reduction in network density of these siloxanes within the polyimide. At higher levels of substitution the reduction in elongation at break and tensile strength may be due to both a deterioration in interfacial adhesion and a reduction in crosslinking density of the dispersed siloxane-rich particles. Possible changes in the configurations of the polyimide chains in the main phase may have to be considered as additional factors responsible for the observed variations in mechanical properties (see later).

Coefficients of thermal expansion (CTEs)

In *Figure 7* are shown typical variations in CTE values with temperature for films of polyimide and the corresponding compatibilized ceramer containing 25% (w/w) equivalent SiO_2, including the effect of different levels of residual moisture. Separate experiments have shown that the CTE values obtained are reproducible after the film is cycled from room temperature to 250°C in the thermomechanical apparatus, and hence this temperature-cycling procedure was used in all subsequent tests. One notes that for both systems the rate of

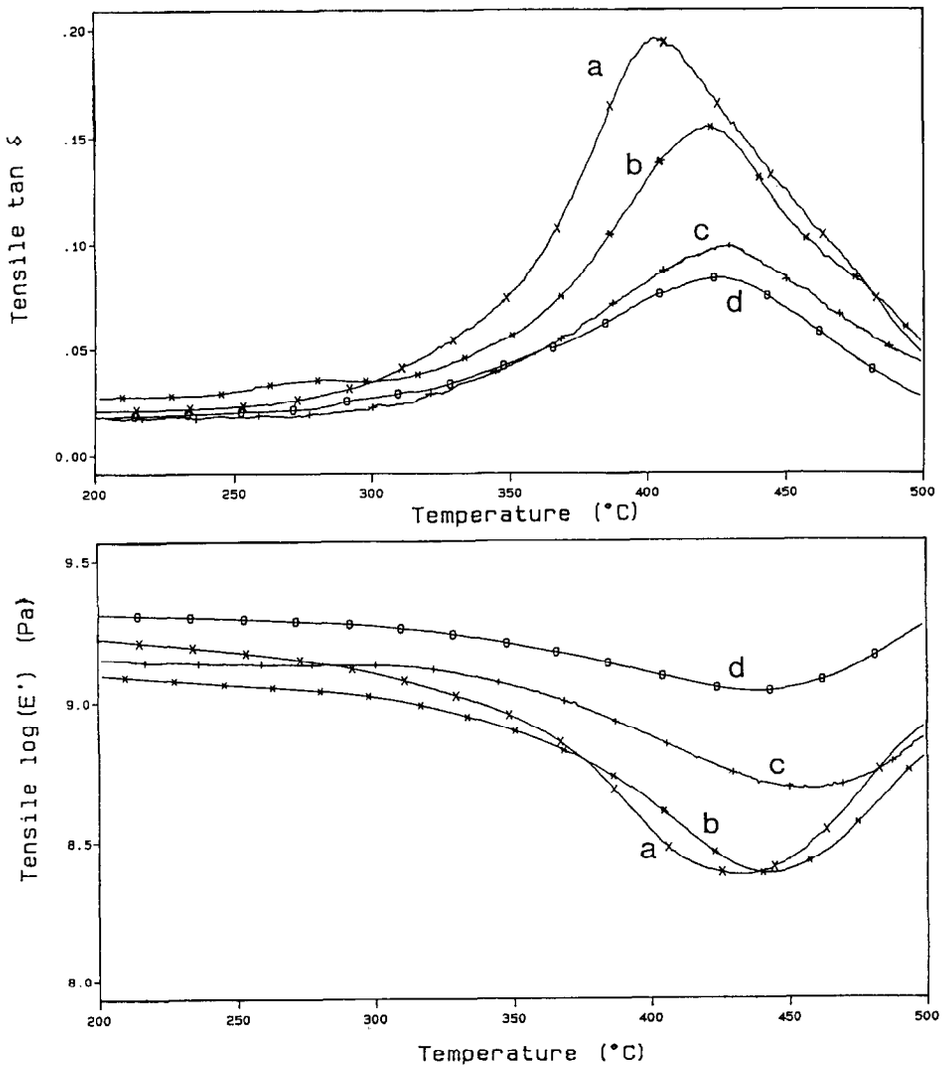

Figure 4 Dynamic mechanical spectra of (a) the polyimide, (b) the non-compatibilized ceramer S with 25% (w/w) SiO_2, (c) the compatibilized (co-continuous) ceramer SE_2 with 25% (w/w) SiO_2 and (d) the compatibilized (co-continuous) ceramer SE_2 with 35% (w/w) SiO_2

increase of the CTE with temperature is greater when residual moisture is present in the film, owing to the volumetric contraction resulting from the desorption of moisture. In the case of ceramers, however, the contraction due to the loss of water can occur at a faster rate than the natural volumetric expansion resulting from the increase in internal energy of the molecular chains. This is believed to be the cause, therefore, for the negative CTE values observed for ceramers containing residual water.

Work carried out on silica gels[31–34] has shown that for temperatures up to 400°C, hydration or dehydration occurs readily and reversibly, and at temperatures above 170°C even the water chemisorbed on the surface of the interconnected particles is desorbed through further condensation reactions. The sorption or desorption of water was found to take place through large volumetric changes particularly in cooling or heating cycles below 250°C[35]. From quantum calculations Zerner *et al.*[36] have estimated that the relative linear changes in silica gels associated with a 1% water absorption or desorption are around 140 ppm compared with 60 ppm for the natural thermal expansion resulting from the increase in internal energy. This analogy with respect to moisture absorption or desorption behaviour provides convincing evidence for the porous nature of the siloxane phase in these polyimide–silica gel hybrids.

The curves in *Figure 8* illustrate the large reduction in thermal expansion which results when the morphology of the dispersed silica component of the ceramers changes from particulate to co-continuous. This effect becomes even more pronounced at temperatures above the T_g of the polyimide and is in concordance with the greater suppression of α-relaxations revealed in the dynamic mechanical tests (*Figure 4*).

In *Figure 9* it is shown, on the other hand, that with the re-establishment of a particulate microstructure for the dispersed silica gel phase through partial substitution of TEOS with DMES, the CTE values increase again owing to the loss of continuity of the silica phase and possibly also through the reduction in its crosslinking density. It is important to bear in mind that these data were obtained on dried samples and therefore interfering effects from moisture have to be excluded.

The thermal expansion behaviour of polyimide films, however, is affected considerably by the constraints

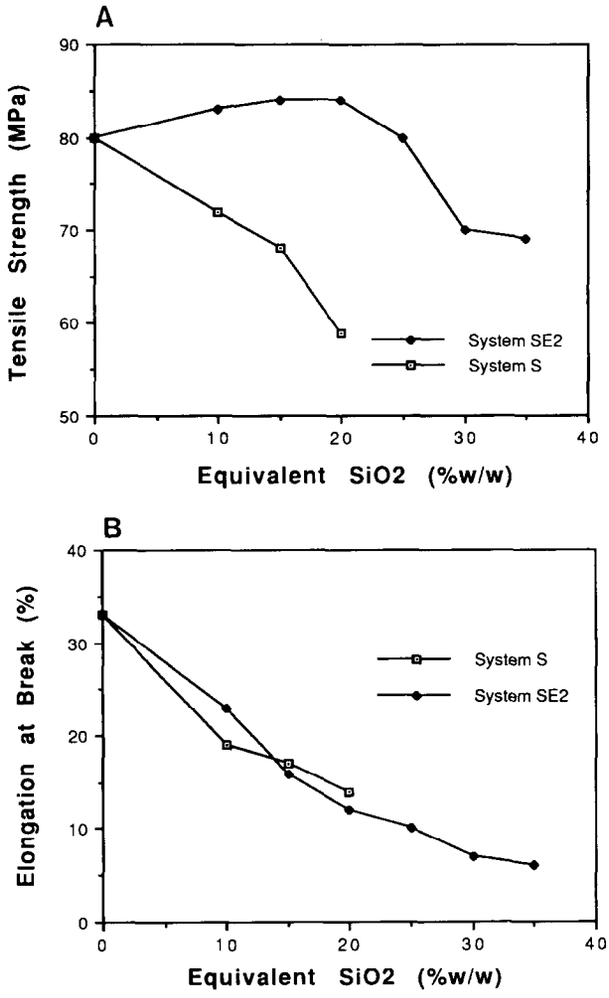

Figure 5 Variation of the mechanical properties of non-compatibilized (system S) and compatibilized (system SE_2) ceramers as a function of equivalent SiO_2 content (solutions mixed for 4 h at 80°C prior to casting films): (A) tensile strength; (B) elongation at break

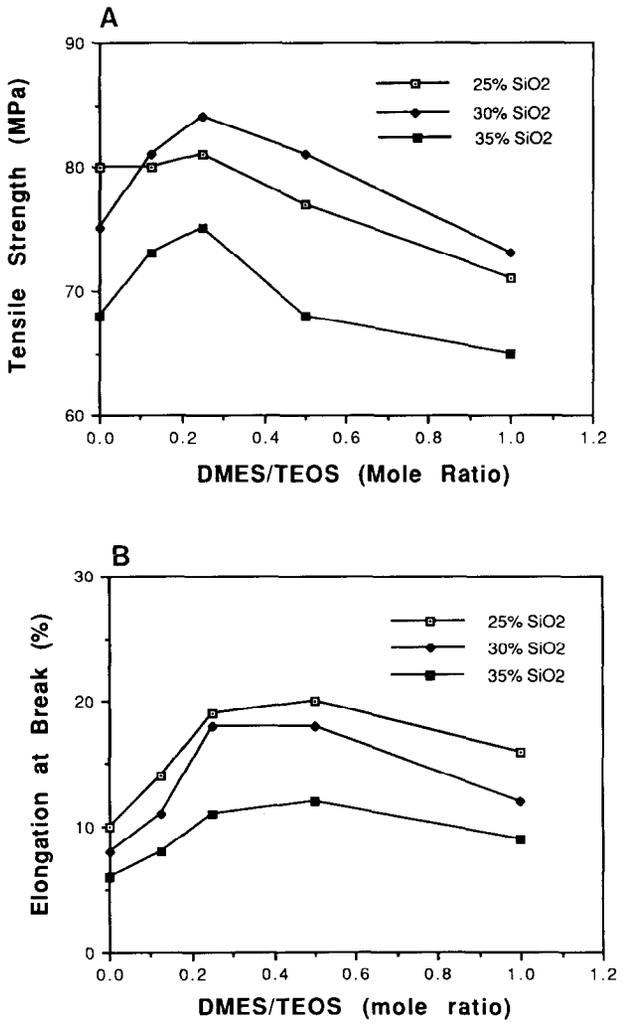

Figure 6 Effects of substitution of TEOS with DMES on the mechanical properties of compatibilized ceramers containing different amounts of equivalent SiO_2: (A) tensile strength; (B) elongation at break

imposed during imidization. In *Figure 10* is shown the CTE variation with temperature for films imidized in the free state and under biaxial constraints, whereas *Figure 11* shows the effect of constraining the film through interfacial adhesion by carrying out the imidization on two different substrates. In both cases the constraints produce biaxial orientation which relaxes when the temperature is increased above the glass transition temperature of the polymer, as evidenced by the negative slope of the CTE curve. The data in *Figure 11* not only provide the experimental evidence for the anticipated correlation between the molecular orientation in the film and the surface energy of the substrate but also show that the surface energy of the substrate does not have to be particularly high to restrict molecular relaxations in the film during imidization.

It is worth noting that the surface energy value quoted for glass (70 mJ m^{-2}) corresponds to the value obtained for a hydrated surface, so it is equivalent to the surface energy of water. A substantial amount of chemisorbed water is expected to remain adsorbed on the surface of the glass in the range of temperatures used for the curing of the films[31–34], as mentioned earlier.

In *Figure 12* are shown plots of the difference in thermal expansion data between polyimide films produced without constraints and those imidized on a glass substrate for films cured at different temperatures. The curves reveal that the level of orientation in the supported films increases with decreasing curing temperature and suggest that relaxation of the orientation in the unconstrained film takes place largely prior to imidization. From this it can also be inferred that the presence of residual solvent before imidization will facilitate molecular relaxation and reduce the level of orientation in the final film. Support for this interpretation was obtained from experiments carried out on films produced as one-layer and three-layer systems, respectively, for both polyimide and ceramer films about 50 μm thick. The one-layer films were produced by the usual procedure used for films imidized in the free state, i.e. dried on the support at 100°C, peeled and then imidized in successive curing steps. The three-layer films were produced by drying very rapidly each layer (2 min at 180°C) while still supported and subsequently imidizing the laminated film by the usual stepwise curing procedure. The three-layer films were always found to exhibit lower thermal expansion values (40–60%) and higher tensile strength (20–30%), both being a clear manifestation of a higher

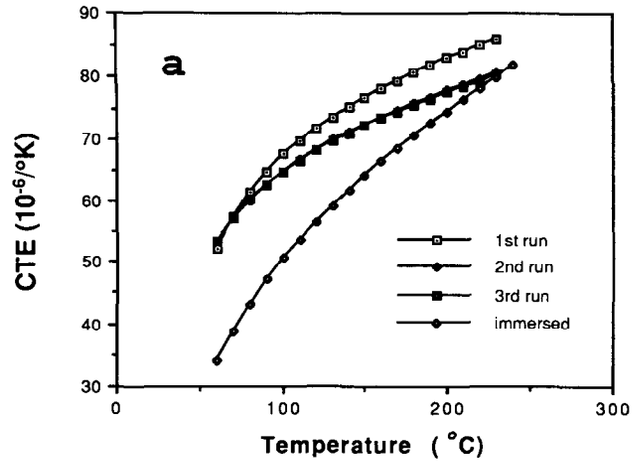

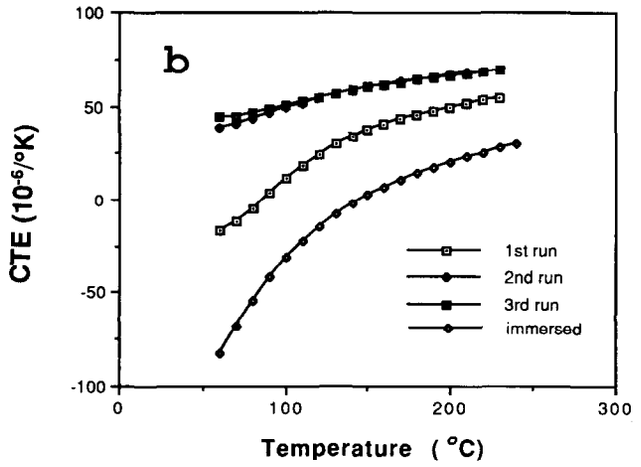

Figure 7 Effects of temperature cycling (from 25 to 250°C) and water immersion (2 h at 80°C) on the coefficient of thermal expansion: (a) polyimide; (b) compatibilized ceramer SE_2 containing 25% (w/w) equivalent SiO_2

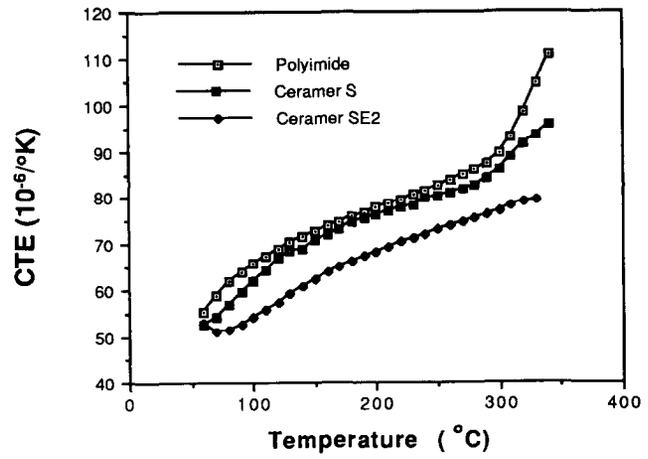

Figure 8 Effects of compatibilization on the coefficient of thermal expansion of ceramers containing 25% (w/w) equivalent SiO_2

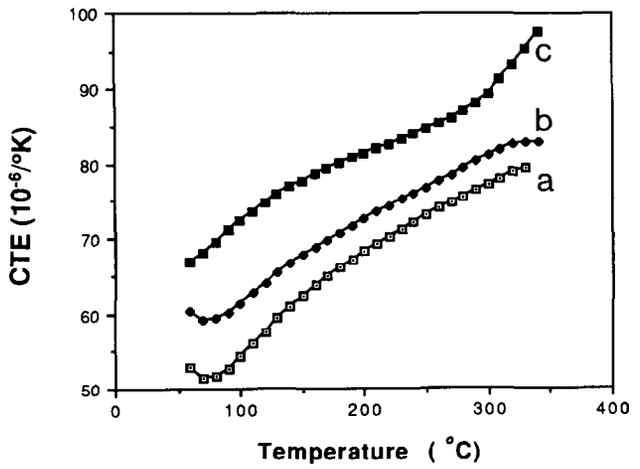

Figure 9 Effects of partial replacement of TEOS with DMES on the coefficient of thermal expansion of compatibilized ceramers containing 25% (w/w) equivalent SiO_2 (for compositions see *Table 1*): (a) system SE_2; (b) system D_5E_2; (c) system D_3E_2

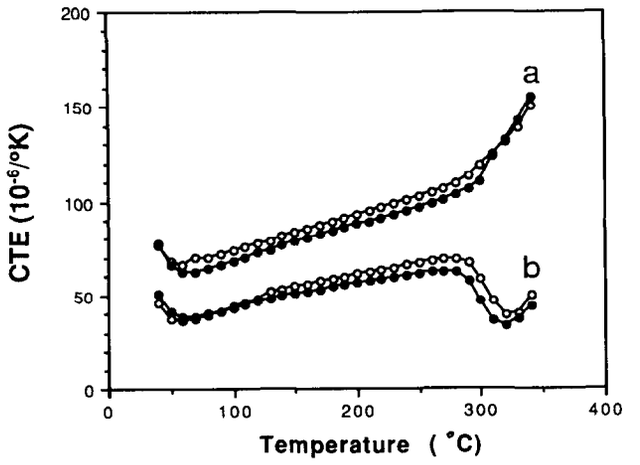

Figure 10 Effects of biaxial constraints during the imidization of the polyamic acid on the coefficient of thermal expansion (open circles, coating direction; closed circles, transverse direction): (a) films imidized in the free state; (b) films imidized under pressure

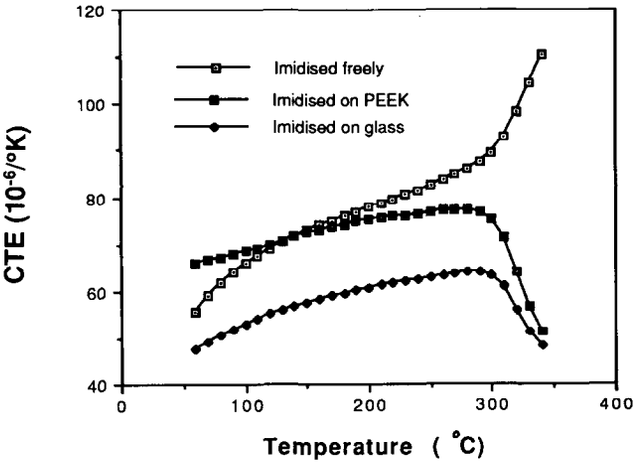

Figure 11 Effects of the nature of the substrate in the production of polyimide films on the coefficient of thermal expansion

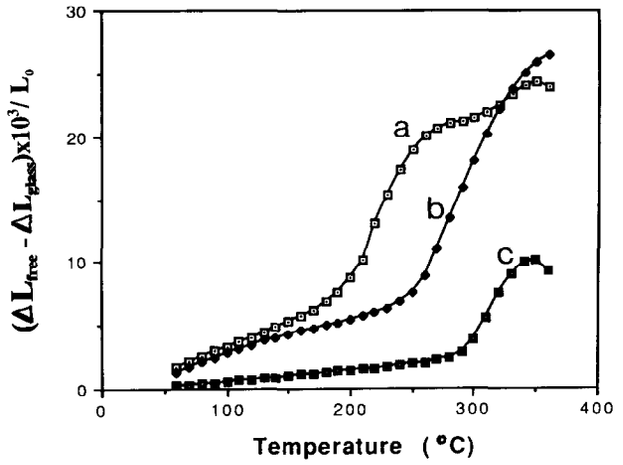

Figure 12 Effect of the imidization temperature of the polyamic acid on the difference in linear expansion between films imidized in the free state and films imidized on glass slides: (a) imidization temperature of 200°C; (b) imidization temperature of 250°C; (c) imidization temperature of 300°C

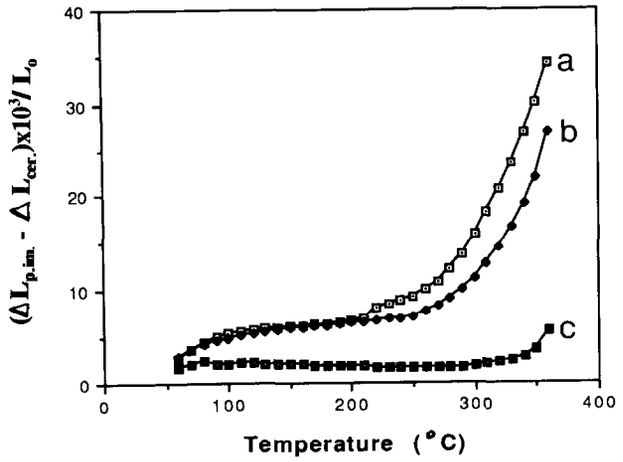

Figure 13 Effect of the imidization temperature on the difference in thermal expansion between the polyimide and a compatibilized ceramer (system SE_2 containing 25% (w/w) equivalent SiO_2): (a) imidization temperature of 200°C; (b) imidization temperature of 250°C; (c) imidization temperature of 300°C. Both systems were imidized without external constraints

level of molecular orientation. This is explained by the rapid volatilization of the solvent in the production of the three-layer films which reduces the extent of molecular relaxations prior to and during the imidization reactions. It is worth noting that the increased orientation obtained in films produced by the multiple layering technique is consistent with the higher orientation observed for thin films by Jon *et al.*[37] Both results indicate a direct relationship between residual orientation and the rate of evaporation of the solvent prior to imidization.

In *Figure 13* are shown plots of the difference in linear thermal expansion with temperature between polyimide films and ceramer films containing 25% (w/w) co-continuous silica domains. In both cases the films were imidized in the free state, i.e. without external constraints. The curves show that the difference in thermal expansion between the two systems increases with decreasing imidization temperature, which is in concordance with the behaviour depicted previously with

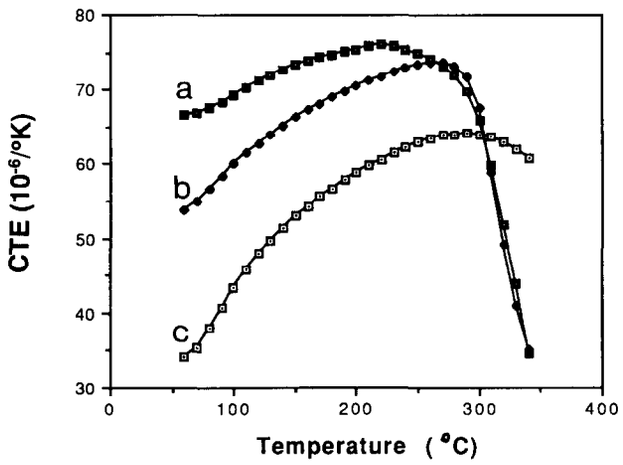

Figure 14 Comparison of the effects of internal and external constraints during imidization on the coefficient of thermal expansion of the polyimide and some ceramers (imidization temperature of 300°C): (a) laminated polyimide–silica–polyimide films (five layers; polyimide outer layers, silica inner layers); (b) polyimide films imidized on glass slides; (c) ceramer SE_2 films (containing 35% (w/w) SiO_2) imidized in the free state

respect to the data in *Figure 12*. From these observations it is deduced that the reduction in thermal expansion associated with the incorporation of co-continuous silica domains within a polyimide matrix in producing hybrid systems is partially due to the development of molecular orientation within the polyimide.

The deduction regarding the major role of the molecular orientation of the polyimide phase in depressing the thermal expansion coefficient of hybrid films finds support from the data presented in *Figure 14*, which shows a comparison of the variations in the thermal expansion coefficient with temperature between (1) a polyimide film cured on a glass substrate, (2) a ceramer film containing 35% (w/w) co-continuous silica domains and (3) a five-layer laminated film consisting of two outer layers with one inner layer of polyimide film and two inner layers of silica film of similar chemical composition as in the ceramer. One observes a remarkable similarity between the three systems; in particular, one notes in every case the relaxation of the orientation of the polyimide component upon reaching its glass transition temperature.

Furthermore, one observes a considerably greater efficiency for the hybrid material in reducing thermal expansion as compared with the equivalent laminated system, bearing in mind that the volumetric ratios of the two phases are about the same. If the reduction in thermal expansion resulted entirely from stress transfer between the two phases, i.e. reinforcement by the silica gel phase, the two systems would be approximately equivalent in view of the prevailing isostrain conditions imposed by the continuity of the phases. Hence the discrepancy between the two systems has to be attributed to a difference in the level of molecular orientation within the polyimide phase, which is expected to increase as the periodic distance between the co-continuous phases becomes smaller.

CONCLUSIONS

This study has highlighted some important features of the structure and properties of polyimide–silica hybrids

which can be summarized as follows.

1. Compatibilization of a silicate 'sol', obtained from hydrolysis and condensation reactions of a tetraethoxysilane solution, with a polyamic acid solution can be achieved by the incorporation of small amounts of γ-glycidyloxypropyltrimethoxysilane to produce hybrid materials exhibiting a finely dispersed co-continuous phase morphology. Partial replacement of the tetraethoxysilane component with dimethylethoxysilane (a non-polar network modifier) causes the precipitation of fine silica-rich particles which are smaller than those observed under conditions in which compatibilization has not taken place. These two morphologies are typical of spinodally separated mixtures, differing from each other in the extent of phase connectivity.
2. The type of prevailing morphology, i.e. co-continuous phases or dispersed particles, affects the level of interaction between the two phases and the resulting physical properties. The co-continuous phase morphology is much more effective in suppressing molecular relaxations, producing a larger reduction in the coefficient of thermal expansion. The dispersed particle morphology, on the other hand, gives higher mechanical strength and ductility. The lower amount of molecular silica network within the continuous polyimide phase and the extent of residual orientation of the polyimide chains are believed to play an important role with respect to both thermal expansion and mechanical properties.

ACKNOWLEDGEMENTS

We are grateful to Pirelli plc for providing financial support for this project. We wish to thank Gary Foster and John Duncan of Polymer Laboratories Ltd for their assistance with the dynamic mechanical tests.

REFERENCES

1 Brinker, C. J. and Scherer, G. W. *J Non-Cryst. Solids* 1985, **70,** 301
2 Yoldas, B. E. *J. Mater. Sci.* 1979, **14,** 1843
3 Mackenzie, J. D. *J. Non-Cryst. Solids* 1982, **48,** 1
4 Fegley Jr, B., Barringer, E. A. and Bowen, H. K. *J. Am. Ceram. Soc.* 1984, **67,** 113
5 Hardy, A., Gowda, G., McMahan, T. J., Riman, R. E., Rhine, W. E. and Bowen, H. K. in 'Ultrastructure Processing of Advanced Ceramics' (Eds J. D. Mackenzie and D. R. Ulrich), Wiley, New York, 1988
6 Fegley Jr, B., White, P. and Bowen, H. K. *Am. Ceram. Soc. Bull.* 1985, **64,** 1115
7 Rabinovich, E. M., MacChesney, J. B., Johnson Jr, D. W., Simpson, J. R., Meagher, B. W., Mimarcella, F. V., Wood, D. L. and Sigety, E. A. *J. Non-Cryst. Solids* 1984, **63,** 155
8 McCreight, L. R., Ranch Sr, H. W. and Sutton, W. H. 'Ceramic Fibres and Fibrous Composite Materials', Academic Press, New York, 1965
9 Hinz, P. and Dislich, H. *J. Non-Cryst. Solids* 1986, **82,** 411
10 Mohallem, N. D. S. and Aegerter, M. A. *J. Non-Cryst. Solids* 1988, **100,** 526
11 Yamame, M., Inoue, S. and Yasumoori, A. *J. Non-Cryst. Solids* 1984, **63,** 13
12 Brinker, C. J., Keefer, K. D., Schaefer, D. W., Assink, T. A., Kay, B. D. and Ashley, C. S. *J. Non-Cryst. Solids* 1984, **63,** 45
13 Pope, E. J. A. and Mackenzie, J. D. *J. Non-Cryst. Solids* 1986, **87,** 185
14 Sakka, S. and Kamiya, K. in 'Emergent Process Methods for High Technology Ceramics' (Eds P. F. Davis, H. Palmour and R. L. Porter), Plenum Press, New York, 1989
15 Mackenzie, J. D. in 'Science of Ceramic Chemical Processing' (Eds L. L. Hench and D. R. Ulrich), Wiley, New York, 1986, p. 113
16 Aelion, R., Loebel, A. and Eirich, F. *J. Am. Chem. Soc.* 1950, **72,** 5705
17 Hench, L. L. and West, J. K. *Chem. Rev.* 1990, **90,** 33
18 Wilkes, G. L., Orler, B. and Huange, H. H. *Polym. Prepr.* 1985, **26,** 300
19 Huang, H. H. and Wilkes, G. L. *Polymer* 1989, **30,** 2001
20 Brennan, A. B., Rodrigues, D. E., Wang, B. and Wilkes, G. L. in 'Chemical Processing of Advanced Materials' (Eds L. L. Hench and K. West), Wiley, New York, 1992, p. 807
21 Nandi, M., Conklin, J. A., Salviati Jr, L. and Sen, A. *Chem. Mater.* 1990, **2,** 772
22 Nandi, M., Conkliu, J. A., Salviati Jr, L. and Sen, A. *Chem. Mater.* 1991, **3,** 201
23 Spinu, M., Brennan, A. B., Rancourt, K., Wilkes, G. L. and McGrath, K. E. *Mater. Res. Soc. Symp. Proc.* 1990, **175,** 179
24 Morikawa, A., Iyoku, Y., Kakimoto, M. and Imrai, Y. *Polym. J.* 1992, **24,** 107
25 Morikawa, A., Iyoku, Y., Kakimoto, M. and Imrai, Y. *J. Mater. Chem.* 1992, **2,** 679
26 Mascia, L. and Kioul, A. *J. Mater. Sci. Lett.* 1994, **13,** 641
27 Kioul, A. and Mascia, L. *J. Non-Cryst. Solids* 1994, **175,** 169
28 Yamanaka, K., Takagi, Y. and Inoue, T. *Polymer* 1989, **30,** 1839
29 Nakanishi, K. and Soga, N. *J. Am. Ceram. Soc.* 1991, **74,** 2518
30 Iyoku, Y., Kakimoto, M. and Imai, Y. *High Perform. Polym.* 1994, **6,** 95
31 Benesi, H. A. and Jones, A. C. *J. Phys. Chem.* 1957, **63,** 179
32 Hockey, J. A. and Pethica, B. A. *Trans. Faraday Soc.* 1961, **57,** 2247
33 Kriesler, A. V. 'Structure and Properties of Porous Materials', Vol. 10, Butterworth, London, 1958, p. 195
34 McDonald, R. S. *J. Phys. Chem.* 1958, **62,** 1168
35 Zhu, B. F., Wang, F. and Hench, L. L. in 'Proceedings of the 4th Conference on Ultrastructure Processing of Ceramics, Glasses and Composites', Tucson, AZ, 1989
36 Zerner, M. C., Loew, G. H., Kirchner, R. F. and Mueller-Westerhoff, U. T. *J. Am. Chem. Soc.* 1980, **102,** 589
37 Jon, J.-H., Huang, P.-T., Chen, H.-C. and Liao, C.-N. *Polymer* 1992, **23,** 967